Ann. Anim. Sci., Vol. 25, No. 2 (2025) 585–595 *DOI: 10.2478/aoas-2025-0009*

sciendo

IDENTIFICATION OF GENES RELATED TO FAT DEPOSITION AS CANDIDATES FOR ER STRESS BASED ON COMBINED RNA-ATAC SEQUENCING ANALYSIS

Katarzyna Piórkowska[1♦], Kacper Żukowski[2], Wojciech Witarski[1], Katarzyna Kowalska[1], Katarzyna Ropka-Molik[1], Mirosław Tyra[3]

[1]Department of Animal Molecular Biology, National Research Institute of Animal Production, 32-083 Balice n. Kraków, Poland
[2]Department of Cattle Breeding, National Research Institute of Animal Production, 32-083 Balice n. Kraków, Poland
[3]Department of Pig Breeding, National Research Institute of Animal Production, 32-083 Balice n. Kraków, Poland
♦Corresponding author: katarzyna.piorkowska@iz.edu.pl
ORCID:
Katarzyna Piórkowska – https://orcid.org/0000-0002-4368-9624
Kacper Żukowski – https://orcid.org/0000-0002-5690-3634
Wojciech Witarski – https://orcid.org/0000-0001-8957-8623
Katarzyna Kowalska – https://orcid.org/0000-0002-0559-4480
Katarzyna Ropka-Molik – https://orcid.org/0000-0002-8555-0495
Mirosław Tyra – https://orcid.org/0000-0001-8221-3461

Abstract

Endoplasmic reticulum (ER) stress is associated with obesity as this state challenges lipid and carbohydrate metabolisms, resulting in glucolipotoxicity and endoplasmic reticulum dysfunction. It can be induced by excessive ectopic fat accumulation, rising blood glucose levels or meta-inflammatory factors, which disturb the liver's numerous pathways favoring hepatic lipogenesis. In the present study, it was attempted to identify liver molecular processes associated with fat deposition in pigs based on combined RNA-ATAC-seq analysis. The pig groups used in the present study were significantly different in terms of subcutaneous and visceral fat deposition; they belonged to a native Polish breed and were not under selection pressure. Based on RNA-ATAC-seq combined analysis, identification was made of 45 significant differentially expressed genes (DEGs) in liver tissue dependent on fat deposition, for which open chromatin regions in transcription start sites were found. The functional analysis pinpointed that 5 of them are involved in the ER stress process (*MANF*, *SELENOS*, *HYOU1*, *PIK3R1*, and *HSPA5*). These five proposed genes expressed in the liver as candidates associated with fat deposition in pigs because ER stress plays a significant role in this organ in molecular process associated with the determination of fat level in the organism, which was previously broadly described in humans.

Key words: ATACseq, liver, endoplasmic reticulum (ER) stress, fat tissue, pig

Domestic pigs (*Sus scrofa*) have undergone long-term selection for lean meat. These treatments have led to significantly decreased fat contents in carcasses, regarding subcutaneous and intramuscular fat types (Tyra and Zak, 2013). Therefore, one of the priorities in pig breeding is to recover the proper fat content, which is strongly associated with meat flavor and its technological properties (Savell and Cross, 1988). Thus, searching for molecular processes related to adipogenesis and fat deposition using pigs as the scientific model is still popular (Ropka-Molik et al., 2020; Sun et al., 2020; Xing et al., 2019).

Endoplasmic reticulum (ER) stress occurs when ER homeostasis is perturbed by the accumulation of unfolded/misfolded proteins or calcium depletion (Malhi and Kaufman, 2011). The liver is a vital metabolic, secretory and excretory organ, where hepatocytes are the predominant cell type playing a significant secretory role. Hepatocytes are enriched in ER and are highly susceptible to ER perturbation and stress. If ER stress is prolonged and restoration to ER homeostasis fails, unfolded protein response (UPR) activation leads to cell death (Liu and Green, 2019). ER stress has been implicated in the pathogenesis of liver diseases such as non-alcoholic fatty liver disease (NAFLD). Moreover, ER stress is strongly associated with obesity as this state challenges lipid and carbohydrate metabolisms, resulting in glucolipotoxicity and endoplasmic reticulum dysfunction (Fernandes-da-Silva et al., 2021). ER stress can be induced by, for example, excessive ectopic fat accumulation, rising blood glucose levels or meta-inflammatory factors, which disturb the liver's numerous pathways favoring hepatic lipogenesis. ER stress is also intensely active in obesity, hepatic steatosis, and diabetes pathogenesis, and has become a potential target to prevent metabolic diseases. Therefore, scientists seek strategies to alleviate ER stress by avoid-

*This study was supported by the statutory activity of the National Research Institute of Animal Production no. 01-18-05-21 and The National Centre for Research and Development in Poland – BIOSTRATEG2/297267/14/NCBR/2016.

ing inflammation, apoptosis, lipogenesis suppression, and insulin sensitivity augmentation.

In the present investigation, a combination of assay for transposase-accessible chromatin (ATAC-seq) and RNA-seq analyses of the liver tissue were used to identify DNA regulatory elements widespread in the *Sus scrofa* genome related to fat deposition molecular process. Pig groups used in the present study significantly differed in subcutaneous and visceral fat deposition. The goal of the present study was to identify crucial differently expressed genes associated with fat deposition mechanisms, for which specific, important open chromatin regions were determined. The study combined RNA and ATAC-seq methods to test transcriptome and transcriptionally active chromatin within lean and fatty pigs. In pig breeding, the knowledge of genome regulation still needs to be improved, making it difficult for researchers to understand and identify causative variants related to complex traits that could be used in genomic prediction in breeding programs. Moreover, epigenetic regulations associated with determining fat storage in pig species must be better understood. In the present report, one of the important liver molecular process was identified that is probably highly associated with increased fat storage in pig carcasses.

Material and methods

Animals

The research biological material was derived from pigs (Złotnicka White) maintained in the Pig Testing Station (PTS) of the National Research Institute of Animal Production.

Seventy five gilts of Złotnicka White were maintained at the weight of 100±2 kg in the PTS, keeping the same feeding and environmental conditions. This part of the study was funded by the National Centre for Research and Development in Poland no. BIOSTRATEG2/297267/14/NCBR/2016. Immediately after slaughtering, liver tissues from all pigs were sampled and stabilized in RNAlater™ Stabilization Solution (Invitrogen™) (gene expression analysis) and media tissue-specific for liver tissue (William's E medium with 1x hepatocyte plating/thawing medium A; Thermo Fisher Scientific) (ATAC-seq analysis). Samples for ATAC-seq after Acutase digestion were frozen in cryotubes with cryoprotectant Cryostor 10 (Stemcell) and Mr Frosty™ Freezing Container to the temperature –80°C and these in RNAlater solution in –20°C. In turn, in the PTS, after 24 hours of cooling, the right half-carcass of all pigs was dissected, and traits associated with fat content were measured. Based on this estimation, 16 pigs were selected and classified into fat or lean groups, 8 per group (Table S1). The results of pig carcass traits of selected pigs were presented in a previous study (Piórkowska et al., 2022).

cDNA, ATAC and DNA library preparation

RNA from liver tissue was isolated using PureLink™ RNA Mini Kit (Invitrogen™). The RIN parameters were estimated by the TapeStation 2200 system and RNA tapes (Agilent). The samples with RIN over 7 were acceptable. cDNA libraries for liver tissue were prepared by TruSeq RNA Sample Preparation Kit v2 (Illumina).

Frozen liver cells for ATAC libraries were thawed, washed, and centrifuged. A vitality test was performed using 0.4% trypan blue nucleus stain (Sigma Aldrich) and calculation based on prepared software (Chrobociński et al., 2022). To further analysis, liver cell samples should be performed with 80% vitality. Due to this restriction, 2 samples were removed, and the number of samples in each group was reduced. The ATAC library preparation was performed with a modified Buenrostro et al. (2015) procedure. Based on Scepter2 (Millipore), and 60 mm aperture sensors, 50,000 cells in 1.5 ml were lysed in Lysis Buffer that contained 10 mM Tris.Cl, pH 7.4, 10 mM NaCl, 3 mM $MgCl_2$, 0.1 % (v/v) Igepal® following Buenrostro et al. (2015). Then the transposition reaction was performed according to TruePrep™ DNA Library Prep Kit V2 for Illumina® protocol (Vazyme). The ATAC-seq libraries were double indexed (TruePrep Index Kit V2 for Illumina TD502, Vazyme). Special primers (P1-AATGATACGGCGACCACC and P2-GTCTCGTGGGCTCGGAGA) were used according to the Buenrostro et al. (2015) protocol to avoid the cessation of amplification prior to saturation. The ready libraries were purified using AMPure® XP Beads (Beckman). The final concentration was checked by TapeStation2000 (Agilent) and using Quibit 2.0 (Invitrogen™). The ATAC libraries were divided into two fractions, A and B suggested by Milani et al. (2016) and Yan et al. (2020). Fraction A corresponds to that within the nucleosome-free region (NFR) (library size 175–250 bp, insert <100 bp) and fraction B being that with mono-, di, and tri-nucleosomes (library size 250–625 bp, insert ~ 200, 400, 600 bp). This separation was done using ready-to-use 10% Novex™ TBE Gels on the XCell SureLock® Mini-Cell (Invitrogen, Carlsbad, USA) in 0.5% TBE and QIAquick Gel Extraction Kit (Qiagen). For each pig chosen for fat and lean groups, DNA was isolated from liver tissue to prepare naked transposed DNA libraries based on TruePrepTM DNA Library Prep Kit V2 for Illumina® protocol (Vazyme). Results obtained based on DNA libraries were used as internal control to determine the background level of intrinsic accessibility of genomic DNA and correct for any Tn5 transposase sequence cleavage bias (Milani et al., 2016). Quality control of cDNA and ATAC libraries after preparation was performed by Qubit Fluorometer (Invitrogen) and a TapeStation 2200 system (D1000 tapes, Agilent). To work on frozen and thawed liver cells during preparation of ATAC libraries, there have been applied a few special control steps: control of the lysis stage (1) – normal procedure but without adding Tn5 transposase, after ATAC library preparation – control step for the presence of genomic DNA not associated with open chromatin regions, (2) – *GAPDH* promoter enrich amplification – F-TTCCTGGGTCACTACCGAAG, R GGGCAGTGGACTAGGAGGAG and two desert DNA regions (non-

coding genes), region 1 F-TCTGGAAGAGTCTC-CTAAAGCAA, R-GGGCTTCATGATGCTTGTCT and region 2 F- GGCCCAGGAGGTTCTATGAC, R-GCT-GAAGGACAGCTTTGGAG. These special primer pairs should amplify promoter *GAPDH* gene regions in both ATAC libraries and DNA isolated from the liver. cDNA, ATAC-seq and DNA libraries were sequenced in 150PE cycles on a HiSeq 3000 System (Illumina, San Diego, CA, USA) in the outdoor institution (Admera Health Biopharma Services).

ATAC-seq raw data was processed using Flexbar, NGmerge, BWA. Filtration for aligned reads/marking duplicates was performed by samtools, samjdk, picard, own prepared scripts and peak calling analysis has been performed by Genrich (threshold – signal value 200), as negative control results from DNA libraries were included. Ensembl Variant Effect Predictor (VEP) (Sscrofa11.1, GCA_000003025.6, Ensembl 106: Apr 2022) has been used to signal annotation, 5`UTR, 3`UTR, intron, coding sequence, upstream and downstream regions. The statistical analysis involved also information about ATAC signals overlapped transcription start sites (TSSs). The sequence data for ATAC libraries have been submitted to the Gene Expression Omnibus (accession no. GSE199870).

Differential expression analysis for genes and isoforms with corresponding P-values has been performed using a negative binomial generalized linear model in the DeSeq2 package in R/Bioconductor for RNA-seq results (Love et al., 2014). Fold change (FC) >1.2 has been accepted by false discovery rates (FDR, <0.05). For identification of significant ATAC signals, focus has been on the important ATAC peaks that had full representation in only one of the HFD or LFD groups. This approach allowed narrowing the investigation area to the most important gene expression regulation signals. Moreover, TSS and promoter <1 kb peaks were included in the same test.

Validation of RNA-seq results has been performed using qPCR method and 14 genes were tested: *PON3, ACACA2, PCK1, HP, LDHA, CTP1, FASN, FGB, PIK3R1, FADS1, CYP1A1, GYS1, ACAA2*, and *AHSG*. As an endogenous control *RPL29, OAZ1* and *RLP27* have been used. The obtained qPCR results were compared with RNA-seq results by Pearson correlation coefficient and P-value (<0.05) were generated using the SAS Enterprise 7.1 tool. The correlation plot was generated using Excel dot plot with an indicated trend line. Primers and probes were presented in Table S2.

Functional analysis and identification of transcription factor (TF) motifs

The functional annotation clustering of transcriptomic and ATAC results was performed using the functional annotation tool David, Webgestalt and protein–protein interaction (PPI) was assessed using the String database. All other statistical calculations were performed using ANOVA (SAS) and post hoc tests. UCSC Genome Browser was used for visualization of ATAC signals corresponding to significant genes.

All peaks mapped in the TSS and promoter <1 kb regions were aligned to isoforms corresponding to genes and were searched for TF motifs using PROMOv3.

Results

Liver transcriptome profiling dependent on subcutaneous fat (SF) deposition

The average numbers of raw reads detected per sample and after filtration were 60,666,131 and 59,144,631, respectively. After mapping to the pig reference genome (Sscrofa11.1 GCA_000003025.6 assembly), the average exonic rate was 76%, the intronic rate was 14.7%, and the intergenic rate was 8.2%. The heatmap based on the DEGs shows clustering into low- and high-fat pig groups (Figure 1 a). One sample was not included in further analysis due to clustering in the opposite FD group.

The liver transcriptome was investigated across groups of pigs that differed in fat deposition level. It was shown that 364 genes were regulated (showing >1.2 FC and FDR <0.05), dependent on the SF level. The WEBgestalt tool indicated that they were involved in fatty acid metabolism, insulin resistance, glucagon signaling pathways, vitamin B_5 (pantothenate) metabolism, PPARA-activated gene expression, response to elevated platelet cytosolic Ca^{2+}, and the selenium micronutrient network (Figure 1 b).

Validation of RNA-seq results

The RNA-seq results were validated using the qPCR method, and Pearson correlation included 14 genes. qPCR confirmed the RNA-seq outcomes, as a positive correlation was determined for each gene (Table S 3). Lower Pearson coefficients were obtained for the *FASN* gene (P coeff.=0.59), which could be associated with gene complexity, numerous polymorphic variants and slight changes in isoforms compared with the Ensembl data.

ATAC-seq library concentration, QC tests and signal mapping

All control steps were passed: control of lysis stage (i) was properly executed, as was control of the enriched *GAPDH* promoter region (ii).

The Genrich tool identified the signals associated with each sample separately, and at least 5000 signals were identified. All signals were assigned localizations to the 5`UTR, 3`UTR, upstream, downstream, coding sequence and intron regions. Moreover, all signals were checked to determine whether they overlapped with the TSSs. The preliminary statistical analysis showed that in the LFD group, significantly more signals mapped to the 5`UTR regions than in the HFD pigs (Figure 2), and the opposite results were found for ATAC signals associated with intron and intergenic regions, much more signals for intronic and intergenic regions in HFD pigs. Moreover, the length and gene number of signals that overlapped with the TSS were checked and no significant differences between groups were detected.

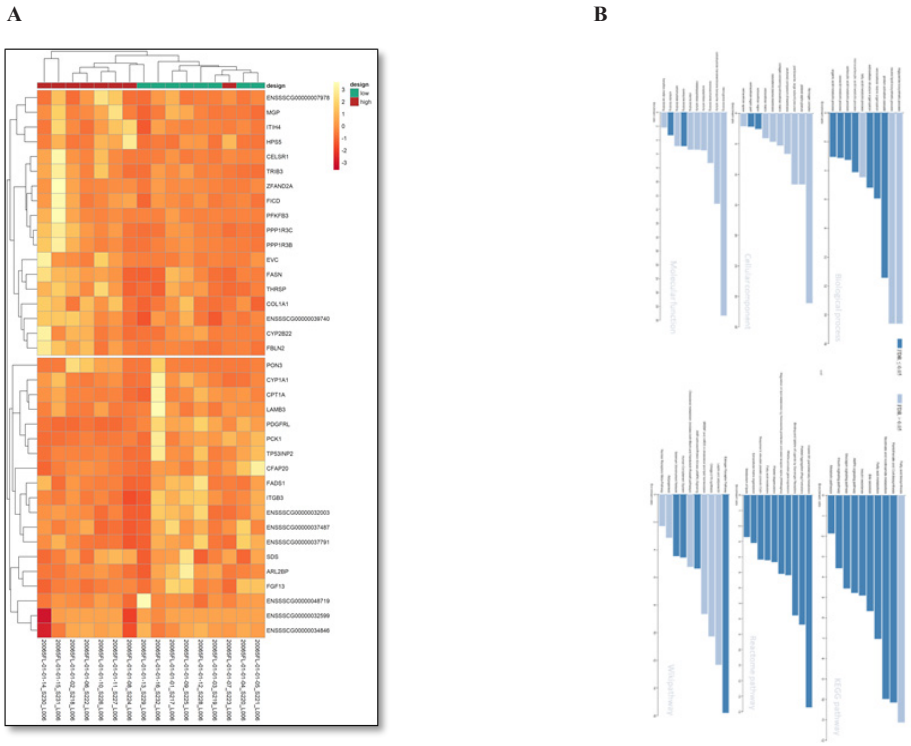

Figure 1. Results for HFD and LFD pig liver samples. **A)** Gene clustering visualized by heatmaps showing genes whose expressions differ between HFD and LFD pigs in liver tissue. Each row refers to a gene, while columns refer to the investigated samples. Upregulated genes are shown in shades of yellow and downregulated in shades of brown. The heatmap for down- and upregulated DEGs was plotted using the R project with the pheatmap package. **B)** Functional analysis performed using the WebGestalt tool. Left side presents GO dependence and right side indicates DEGs involved in the molecular pathways based on different databases

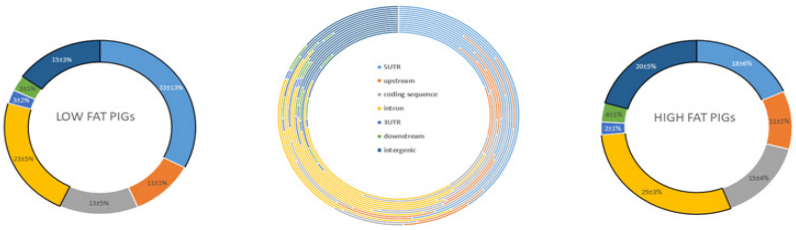

Figure 2. Mapping of ATAC signals to *Sscrofa11.1.100*. **A)** Mean percentage of ATAC signals mapped to particular genome regions for HFD pigs. **B)** Percentage of ATAC signals mapped to particular genome regions for each sample. **C**) Mean percentage of ATAC signals mapped to particular genome regions for LFD pigs. The percentage means that were significant according to ANOVA test between analyzed groups are marked with black frames

Analysis of TSS and promoter <1 kb ATAC signals based on Genrich calculation

There was identified an average of 5425 peaks (corresponding to 12680 genes) and 2194 signals (corresponding to 8840 genes) that overlapped with the TSS and <1 kb promoter region, respectively. Almost 70% of these signals came from A fraction (inserts up to 150 bp). Subsequently, focus was made on ATAC signals only associated with DEGs and these ATAC signals overlapped with 221 DEGs. Nevertheless, these ATAC signals were not present in all samples, therefore in our further consideration, ATAC signals fully represented in only one groups (in the HFD or LFD group) were included, these signals have been called ATAC signals of interest (ATAC SI). This approach narrowed the investigation area to the most critical gene expression regulation signals. Moreover, TSS and promoter <1 kb peaks were included in the same test.

In total, 890 and 2028 ATAC SI corresponding to the TSSs and <1 kb promoter regions were identified in the HFD and LFD groups, respectively. The overlapping DEGs and ATAC SI revealed 45 genes (Figure 3). DAVID ontology (Figure 3 b) and PPI interaction (Figure 3 a) analyses indicated that these genes enriched processes associated with fat cell destination, cholesterol efflux, and ER stress (*MANF, HYOU1, SELENOS, PIK3R1* and *HSPA5*) (Figure 3).

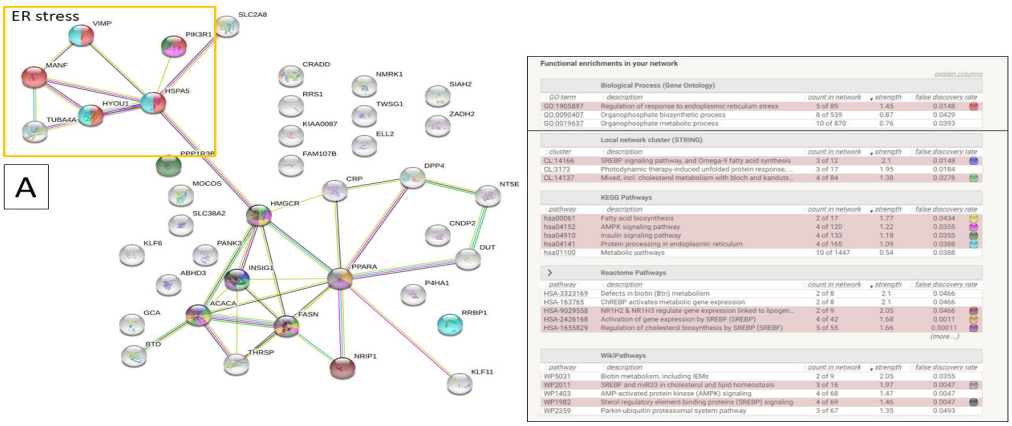

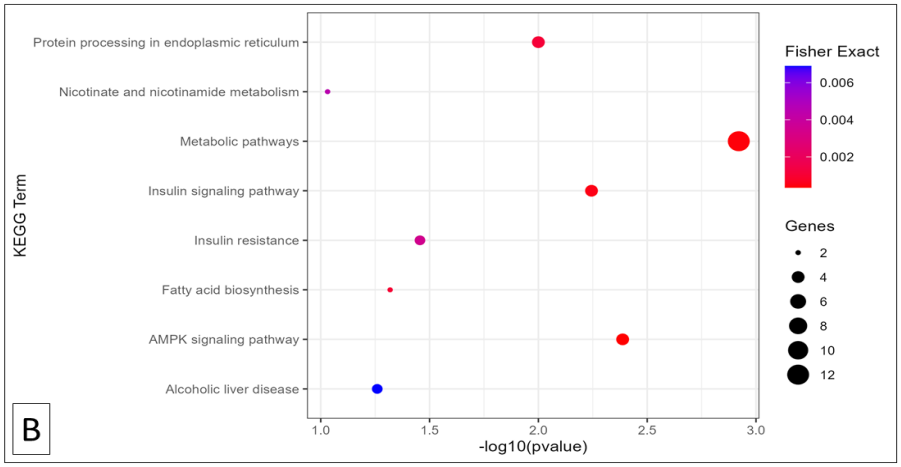

Figure 3. Functional protein association networks for 45 ATAC-DEGs. **A)** PPI analysis presented by STRING **B)** plot generated by ggplot2 R-package. Based on DAVID functional analysis presenting involvement of particular genes in KEGG pathways

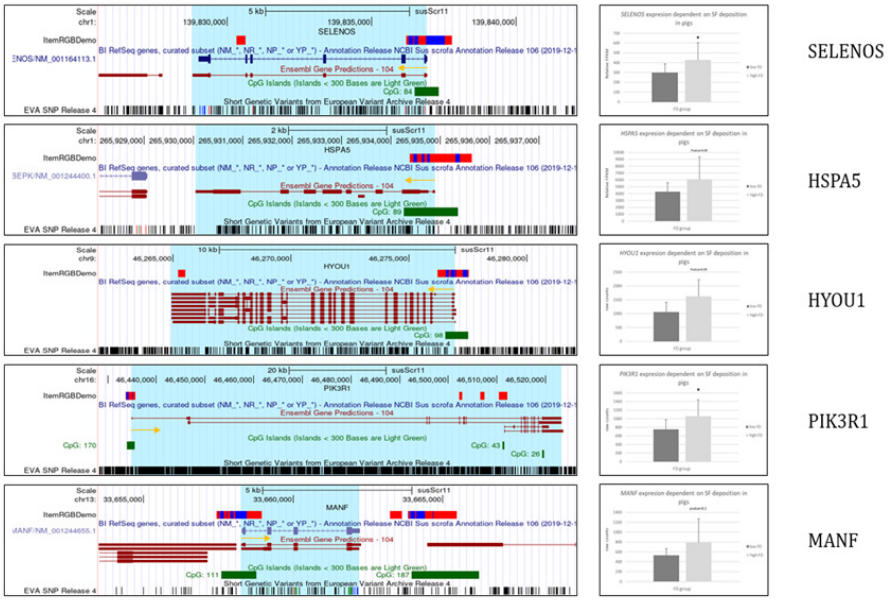

Figure 4. Visualization of ATAC TSS signals using UCSC Genome Browser on Pig Feb. 2017 (Sscrofa11.1/susScr11) and gene expression presented based on raw counts generated by RNA-seq related to ER stress genes. Red and blue colors show ATAC TSS signals for high- and low-FD pig groups, respectively. Ensembl and NCBI gene reference information has been included. In the light blue frame, genes of interest are highlighted. CpG islands are marked in green according to the internal UCSC Genome Browser database. Gene orientation is indicated by yellow arrows

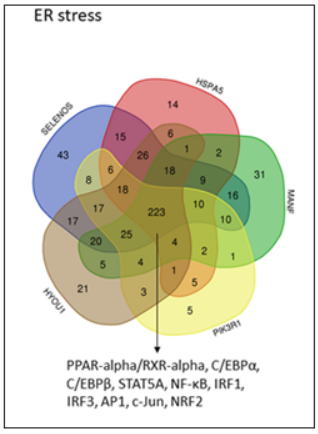

Figure 5. Shared TFs of ATAC signals overlapping TSSs for endoplasmic reticulum stress-related DEGs. Below are indicated TFs that are crucial to regulating the expression of genes in the liver related to fatty liver diseases. PPAR – peroxisome proliferator-activated receptor, RXR – retinoid X receptor, C/EBPa/b – CCAAT/enhancer-binding protein alpha/beta, STAT5A – signal transducer and activator of transcription 5A, NFkB – nuclear factor kappa B, IRF1/3 – interferon regulatory factor 1/3, interferon regulatory factor 1, AP1 – K-box region and MADS-box transcription factor family protein, c-JUN – JUN (CJUN) Jun proto-oncogene, NRF2 – nuclear factor erythroid 2-related factor 2

Table 1. Shared TFs for which binding sites in TSS ATAC signals associated with DEGs ER stress-related were found

Gene name	TF total	TFs associated with fatty liver	Regulated processes
HSPA5,	223	PPAR-alpha/RXR-alpha	Lipid metabolism, inflammation, fibrosis
HYOU1,		C/EBP-alpha	Lipid metabolism
MANF,		C/EBP-beta	Lipid metabolism
PIK3R1,		STAT5A	Lipid metabolism
SELENOS		NF-kB	Inflammation
		IRF1	Inflammation
		IRF3	Inflammation
		AP1	Inflammation, fibrosis
		Nrf2	Inflammation
HSPA5, *HYOU1,* *PIK3R1,* *SELENOS*	18	FOXO3a	Glucose homeostasis
HSPA5 PIK3R1 *SELENOS*	6	XBP1	Metabolic stress
HYOU1 MANF	5	FXR	Lipid metabolism

The RNA-seq analyses for porcine liver show that all genes involved in ER stress were upregulated in the liver, along with increased subcutaneous FD (Figure 4). Moreover, the visualization (yielded by the UCSC Genome Browser combined with CpG island information) reveals that every TSS ATAC signal was strongly correlated with the occurrence of CpG islands.

In the PROMO v3 analysis, DEGs were included for which ATAC signals overlapping the TSS or located in promoter region <1 kb were found. Then, identification was made of the shared TFs of ATAC signals overlapping TSSs for DEGs that enriched the ER stress pathway (Table 1, Figure 5). In Figure 5, the arrows indicate TFs for ER-related genes that are crucial to regulating the expression of genes in the liver related to fatty metabolism (Steensels et al., 2020). Table 1 lists the TFs for ER-related genes that play a significant role in the liver during fat deposition and adipogenesis, and their involvement in particular molecular processes or pathways (Steensels et al., 2020).

Discussion

ATAC-seq analysis enables the identification of open chromatin by generating ATAC signals or peaks, which correspond to gene expression-regulatory elements. Besides the location of the identified peaks, it can obtain sequence information and check for potential TF binding to these regions, suggesting possible transcriptional regulations. In the present study, we performed a combined RNA-ATAC-seq analysis of liver tissue, which was dependent on SF deposition in pigs, to assess the potential capacity of TF regulation to play a significant role during fat storage.

In the experiment, wherein ATAC signals for DEGs were assessed, we observed 45 significant genes that may play a vital role in fat metabolism. Our functional analysis indicated that they could be involved in the regulation of fat cell destination and cholesterol efflux, as well as in ER stress (*MANF, SELENOS (VIMP), HYOU1, PIK3R1* and *HSPA5*). ER stress arises with ER homeostasis, and

the liver is highly susceptible to ER stress given its synthetic and other biological functions. Numerous animal models have been used to pinpoint the crucial role of ER stress in the pathogenesis of liver diseases, including NAFLD (Malhi and Kaufman, 2011). The pig groups used in the present study differed significantly in terms of fat levels, both subcutaneous and visceral (Piórkowska et al., 2022). Our study tested the sequences corresponding to the TSS ATAC signals of significant DEGs possibly related to TF binding. Shared binding sites were identified for a few transcription factors, such as PPAR-alpha/RXR-alpha, C/EBPα, C/EBPβ, STAT5A, NF-κB, IRF1, IRF3, AP1, c-Jun and NRF2, which have been previously determined to play a vital role in transcriptional regulation in NAFLD and related processes (Steensels et al., 2020). Steensels et al. (2020) suggested that other TFs are crucial to the metabolic stress process in the liver – IRE1α, eIF2α, ATF4, ATF6 and Xbp1 – and that metabolic stress is strongly related to cellular and ER stresses. These TFs initiate special transcriptional events that resolve ER stress. In the present study, the binding site of Xbp1 was identified in TSS ATAC signals for three candidate genes for ER stress (*HSPA5*, *SELENOS*, and *HYOU1*), which could suggest transcriptional interaction. Xbp1, as a critical liver TF, is induced in response to a high-caloric diet, which subsequently transcribes factors facilitating protein folding and lipogenesis (Lee et al., 2008). Nevertheless, prolonged obesity-induced stress limits Xbp1, aggravates ER stress and leads to insulin resistance (Lee et al., 2011), and the rescue of Xbp1 resulting from additional Xbp1 doses in a high-fat diet mouse model induces improved glucose homeostasis and reduced hepatic steatosis. However, the molecular mechanisms leading to this process remain unclear (Liu et al., 2015). On the other hand, though the binding site for ATF4 was not identified within ATAC signals overlapping TSSs, which does not rule out transcriptional regulation by ATF4, increased *ATF4* expression was observed in the liver correlated with increased fat deposition, which may also suggest possible transcriptional regulation, and the ATF4 binding site can be located beyond the TSS region. In a previous study on NASH (non-alcoholic steato hepatitis) patients, in which NAFLD was observed, elevated ATF4 expression compared to patients with simple steatosis was shown. In turn, in mice on a regular diet, the depletion of $Atf4^{-/-}$ led to attenuated hepatic lipogenesis without affecting hepatic triglyceride production and fatty acid oxidation, which prevented excessive fat accumulation in the liver. This observation was accompanied by a significant reduction in the hepatic expression of *SREBP-1c, PPARγ, FASN* and *ACC* (Xiao et al., 2013). Thus, increased ATF4 expression in fatty pigs may also suggest the crucial role of ATF4 as a TF in hepatic lipogenesis in this species. On the other hand, unresolved ER stress and the prolonged activation of IRE1α TF lead to the activation of inflammatory transcription factors such as NF-κB and c-jun, though in the present study, ER stress in the liver was not measured, so it can be suggested that these events could be ER stress-related, which needs further analysis. Therefore, these TFs related to inflammation may also play a significant role in the liver, as they are associated with increased SF levels (Steensels et al., 2020). The present report has shown that the identified candidate genes for ER stress contain TF motifs in the TSS for NF-κB and c-jun.

Into the pool of the candidate genes for ER stress, for which ATAC signals in the TSS regions were identified, the *MANF* gene was included which encodes the mesencephalic astrocyte-derived neurotrophic factor, which is a secretory protein, localized in the RE lumen (Yang and Gao, 2020). It is an ER stress-responsive protein and plays a vital role in cell protection. In a rat model, recombinant human MANF significantly inhibited ischemia-induced increases in BiP, p-IRE1, and XBP1, preventing neuron loss (Yang et al., 2014). Cell-derived MANF protects against liver inflammation and fibrosis, while hepatocyte-derived MANF prevents hepatosteatosis (Chhetri et al., 2020). During hepatocellular carcinoma (HCC) development, MANF can act as a cancer suppressor by inhibiting the NF-κB/Snail signal pathway (Liu et al., 2020). Moreover, it was observed that MANF supplementation ameliorates several hallmarks of liver aging (Chhetri et al., 2020), including improving age-related metabolic dysfunction. In addition, the literature reports that *MANF* expression in tissues other than the liver is regulated by ATF6 and Xbp1 transcription factors (Lindholm et al., 2008; Mizobuchi et al., 2007). However, in pig liver, this regulation can be associated with regions other than the TSS, especially when ATF6 and Xbp1 involvement in metabolic stress has previously been suggested. In the present study, a positive correlation was observed between *MANF* expression and fat deposition, which could be related to the activation of molecular mechanisms to prevent ER stress induced by excessive subcutaneous fat accumulation; given that the positive correlation between liver and subcutaneous fats content has previously been widely described (Jang et al., 2011), *MANF* can be considered as valuable molecular marker in pig breeding. However, the present study did not investigate whether ER stress in the liver was observed in the fatty pigs based on liver parameters, which can be the subject of further research. Although a reporter for IRE1/XBP1 pathway activation confirmed that obesity elicits ER stress predominantly in the liver (Yoshiuchi et al., 2008), the suggested transcriptional interaction network should be further experimentally tested using cell culturing in future studies.

HYOU1 encodes hypoxia-upregulated 1, belonging to the Hsp70 family, also known as the 150 kDa oxygen-regulated protein (ORP150). *HYOU1* is induced in response to a variety of stimuli, including endoplasmic reticulum stress, hypoxia or glucose deficiency (Kuwabara et al., 1996). In turn, its upregulation is associated with numerous diseases related to endoplasmic reticulum stress, such as diabetes, degenerative neurological diseases and cardiovascular diseases (Wang et al.,

2019). Moreover, a type 2 diabetes study has shown that HYOU1 can improve insulin sensitivity in the liver, but is not implicated in insulin secretion (Rao et al., 2021), and its anti-ER stress and anti-apoptotic effects occur downstream of AMPK signaling in liver cell lines (Sanson et al., 2008). Overall, HYOU1 is considered a chaperon protein for ER, because during ER stress, HYOU1 inhibits apoptosis, maintains calcium homeostasis, and exhibits cytoprotective effects by preventing this kind of stress through the implementation of many molecular mechanisms, such as the phosphorylation of IRE1 and JNK and the downregulation of XBP1, XBP1s and CHOP expression. Moreover, its interaction with ATF6 and IRE1 keeps them inactive, thereby inhibiting UPR. In the liver, *HYOU1* is mainly induced in response to ER stress, for example in Fed–Fast–Refed cycle experiment, as it was tested using a mice model (Ji et al., 2023). In our study, the upregulation of *HYOU1* was identified in the liver, along with increased SF deposition. Zong et al. (2016) showed that inducing *HYOU1* expression recruits Nrf2 and ATF4 transcription factors during thyroid cancer development. The ATAC signal found as overlapped with the TSS *HYOU1* region revealed a motif for Nrf2; in turn, *ATF4* expression was also positively correlated with SF deposition, which suggests a similar approach to regulation as in thyroid cancer development.

Selenoprotein S (SELENOS) belongs to the selenoprotein family, which exhibits a wide range of potentially highly important biological functions, though this remains unclear for nearly half of the members (Pitts and Hoffmann, 2018). However, individual animals in a mouse model with a deficiency of the tRNASec required for selenoproteins synthesis did not survive early embryogenesis (Bösl et al., 1997). Studies in humans reported that the defective expression or function of selenoproteins impinges upon numerous physiological processes in muscular, skeletal, respiratory, neurological and endocrine systems (Schweizer and Fradejas-Villar, 2016). Selenoprotein S is localized in the ER membrane. It has a glycine-rich C-terminal region that mediates binding with VCP (Lee et al., 2014). Thus, SELENOS is also known in the literature as VIMP (VCP-interacting membrane protein) (Ye et al., 2004). SELENOS is highly expressed in the pancreas, adipose tissue, testis, and stomach. It has been identified in a human study that its promoter contains the ER stress element and binding sites for the factor NF-kB. Moreover, *SELENOS* upregulation was observed in response to inflammatory cytokines (Curran et al., 2005), ER stress, and glucose deprivation (Gao et al., 2004). During ER stress, SELENOS is essential to ER-associated degradation (ERAD), whereby this multiprotein complex translocates misfolded proteins across the ER membrane for cytosolic degradation by the UPR system (Lee et al., 2015). In turn, cell culture experiments found that the knockdown of SELENOS impairs cell viability in response to agents that cause ER stress (Rueli et al., 2017). Moreover, it was suggested that SELENOS indirectly implicates Ca^{2+} signaling by maintaining ER homeostasis and its role in ERAD (Pitts and Hoffmann, 2018). In the liver, a higher *SELENOS* expression was found in steatosis. Moreover, in the human liver, increased over 4-fold *VIMP* expression was found after acetaminophen (APAP) or diclofenac (DCF) treatments as the response to injury and activation of repair procedures (Vickers et al., 2018), which was classified as related to ER stress. On the other hand, liver *VIMP* expression level was elevated after selenium supplementation, which was observed in male mice (Capelle et al., 2021). In the present study, an increased *SELENOS* expression was found in the livers of fatty pigs, which could be associated with preventing ER stress. This observation also suggests that ER stress can significantly affect the response to increased SF deposition.

HSPA5 encodes the binding immunoglobulin protein (BiP) (Kampinga and Craig, 2010), and is also a member of the heat shock protein (HSP70) family. It is localized in the ER lumen, which plays the role of a chaperon in the folding and assembly of proteins. During ER stress, it interacts with the transmembrane stress sensor proteins PERK, IRE1 and ATF6, inducing the repression of UPR. BiP contains two structural domains, a nucleotide-binding domain (NBD) and a substrate-binding domain (SBD), which interact and facilitate the translocation of proteins into the ER, folding and holding protein substrates there, as well as initiating UPR and assisting in ERAD (Wang et al., 2017). HSPA5 promotes the degradation of cytotoxic misfolded proteins and cell survival (Wang et al., 2009). HSPA5 is highly expressed in the liver during NAFLD. It has been observed that the new adipokine vaspin, which regulates hepatocyte steatosis, acts via HSPA5, which significantly reduces hepatocyte fibrosis via the activation of AMP-activated protein kinase (AMPK) and decreasing NF-κB gene expression (Abdolahi et al., 2022). Moreover, Rehati et al. (2023), using RIP-Seq assays, demonstrated that HSPA5 immunoprecipitates specific cellular mRNAs such as EGFR, NEAT1, LRP1 and TGFß1, which are important in the pathology of NAFLD, and HSPA5 might play an important role in regulating the alternative splicing of NAFLD-related genes. Our research has identified the increased expression of *HSPA5* in fatty pigs, which could be associated with a similar mode of molecular regulation to that which was presented during NAFLD in the human study. Moreover, binding sites were found for numerous vital liver TFs in ATAC signals; however, in the literature, there is no information about the upstream regulation of the *HSPA5* gene, which may be a target in future studies because motifs of important liver TFs were found in TSS ATAC for the *HSPA5* gene in the present study, which suggests potential regulation.

PIK3R1 encodes subunit 1 of the phosphoinositide-3-kinase regulatory mechanism, which is a heterodimer that consists of an SH2-containing regulatory subunit (p85) and a catalytic subunit (p110) (Ueki et al., 2000). Fruman et al. (2000) showed, using a mouse model, that the deletion of *PIK3R1* in the liver may result in a

marked reduction in insulin-stimulated PI3K activity, with significant reductions in glucose and lipid homeostasis. Overall, PIK3K/Akt signaling pathway regulates numerous cellular activities such as induction of stem cell differentiation, promotion of cell proliferation and inhibition of apoptosis. Wang et al. (2022) indicated that this pathway exerts anti-inflammatory, antioxidant stress, anti-apoptosis and autophagy regulation effects through downstream related targeted pathways and proteins, thus alleviating liver ischemia-reperfusion injury. Therefore *PIK3R1* plays a role in the liver repair procedure in response to different types of injuries. Moreover, it was proved that *PIK3R1* regulates HCC and its expression in HCC tissue is significantly increased compared to normal tissue. This overregulation is associated with proliferation, migration and promotion of apoptosis in HCC cell line (Ai et al., 2018). In addition, the upregulation of *PIK3R1* is described in numerous other human cancers (endometrial, breast, colon and glioblastoma), and its role in tumor progression and metastasis has been confirmed (Ai et al., 2018; Lin et al., 2015). In turn, the PIK3R1 (p85-alpha) can play a significant role in ER stress because disturbing the heterodimerization between p85α (Pik3r1) and p85β (Pik3r2) in response to insulin treatment allows monomers of p85 to interact with XBP-1, which is one of the main regulators of UPR (Park et al., 2010). This interaction entailed an increase in the nuclear translocation of XBP-1s, the spliced form of XBP-1. In ob/ob mice, this interaction is lost, which results in a severe defect in XBP-1s translocation and in the resolution of ER stress; the amelioration of this defect was achieved after inducing p85α and p85β expression (Park et al., 2010). In our study on fatty pigs, increased *PIK3R1* expression was observed in the liver, which suggests the role of ER stress in response to excessive fat deposition, as in human obesity. However, the expression level of *PIK3R2* was not increased in these pigs, which suggests the role of the Pik3r1 monomer before dimerization with p85β, which should be tested in future studies using cell culturing. On the other hand, following the analysis of the TSS ATAC signal of *PIK3R1*, TF binding motifs were found for numerous important TFs related to lipid metabolism in the liver. However, in the previous report by Kim et al. (2014), it was only indicated that *PIK3R1* expression is sensitive to the PPAR-gamma in 3T3-L1 adipocyte cells, and two motifs, known as PPRE regions, were found located 2,000 bp upstream of the *PIK3R1* TSS. Further, *PIK3R1* promoter expression increased, induced by the PPARγ overexpression, which enhanced the insulin-stimulated activation of AKT. In the present study no other ATAC signal located in the upper promoter region was identified, so regulation of PPAR-gamma with fat deposition in the liver is doubtful. However, the binding of the other significant TFs for which motifs were found in the promoter of *PIK3R1* in pigs can be tested in future studies.

The presented ER stress-related genes/proteins interact together, inducing multiple processes. It was observed that siRNA-mediated silencing of MANF showed increased cultured cells sensibility to ER stress-induced death (Apostolou et al., 2008). While, during ER stress, UPR sensors (IRE1, PERK and ATF6) are induced and GRF78 (HSPA5) protein (Dudek et al., 2009) interacts with three UPR sensors and HYOU1 as its co-factor controls its function. ERSE-II (ER stress response element II) is found in ERAD-related components HERPUD1 (homocysteine-inducible, ER stress-inducible, ubiquitin-like domain member 1, also known as HERP) and VIMP (Schulze et al., 2005) and mammaliam MANF is upregulated by ERSE-II expression (Mizobuchi et al., 2007). *HSPA5* and *XBP1* are induced as prosurvival reporters during ER stress (Iurlaro and Muñoz-Pinedo, 2016) and PIK3R1 (p85-alpha) disturbs the heterodimerization between p85α (Pik3r1) and p85β (Pik3r2), where p85 interacts with XBP-1 (Park et al., 2010).

Conclusion

The application of a comprehensive approach combining ATAC and RNA-seq analyses allowed us to pinpoint the metabolic stress processes that occurred in porcine liver and that were crucial for fat deposition. The analyses performed indicate epigenetic modification, which could be strongly associated with fat deposition and suggests a significant role of ER stress in fat accumulation. The proposed candidate genes related to ER stress (*MANF, SELENOS, HYOU1, PIK3R1* and *HSPA5*) should be analyzed in the future in terms of factors determining fat deposition through modifications of pathways in liver tissue. They should also be tested in further studies where ER stress in the liver will be estimated in the fat deposition context. In turn, open reading frame analyses using the available web databases pinpointed which potential TFs can be bound, and where, which suggested transcriptional regulation for important ER-related genes. Moreover, multiple similarities with NAFLD in the human study confirmed that pigs could represent a good animal model for recognizing molecular processes associated with increased fat status. However, future studies applying cell culturing should investigate the potential of transcriptional regulation.

Ethics approval and consent to participate

The research has been performed on biological material derived from pigs maintained and slaughtered in the Pig Test Station (National Research Institute of Animal Production). In the Test Station pigs were slaughtered, dissected and after carcass evaluation, meat was standard intended for consumption. Therefore, our research did not require the approval of Animal Experimentation Committee. All conducted pig trial was approved by the Approving Experiment Committee of the National Research Institute of Animal Production (Kraków, Poland) and the national authority according to the Polish Act on the Protection of Animals Used for Scientific or Educational Purposes of 15 January 2015 (which implements Directive 2010/63/EU of the European Parliament and of

the Council of 22 September 2010 on the protection of animals used for scientific purposes).

Availability of data and materials

The sequence data obtained after RNA-seq analysis were submitted to the Gene Expression Omnibus GEO NCBI (accession no. GSE160436). The sequence data on ATAC libraries have been submitted to the Gene Expression Omnibus GEO NCBI (accession no. GSE199870).

Competing interests

None of the authors has a financial or other relationship with other people or organizations that may inappropriately influence this work.

Author contributions

Conceptualization, K.P.; methodology, K.P., M.T., and K.Ż.; validation, M.T.; formal analysis, K.P., K.Ż., K.K., W.W and K.Z.; investigation, M.T.; resources, K.R.-M.; data curation, K.P. and K.R.-M; writing – original draft preparation, K.P., K.Ż., and K.Z.; writing – review and editing, K.P. and K.R-M; supervision, K.P.; project administration, M.T.; funding acquisition, K.P. and M.T.

References

Abdolahi A., Vahabzadeh Z., Izadpanah E., Moloudi M.R. (2022). Vaspin attenuates steatosis-induced fibrosis via GRP78 receptor by targeting AMPK signaling pathway. J. Physiol. Biochem., 78: 185–197.

Ai X., Xiang L., Huang Z., Zhou S., Zhang S., Zhang T., Jiang T. (2018). Overexpression of PIK3R1 promotes hepatocellular carcinoma progression. Biol. Res., 51: 1–10.

Apostolou A., Shen Y., Liang Y., Luo J., Fang S. (2008). Armet, a UPR-upregulated protein, inhibits cell proliferation and ER stress-induced cell death. Exp. Cell Res., 314: 2454–2467.

Bösl M.R., Takaku K., Oshima M., Nishimura S., Taketo M.M. (1997). Early embryonic lethality caused by targeted disruption of the mouse selenocysteine tRNA gene (Trsp). Proc. Natl. Acad. Sci. USA, 94: 5531–5534.

Buenrostro J.D., Wu B., Chang H.Y., Greenleaf W.J. (2015). ATAC-seq: A method for assaying chromatin accessibility genome-wide. Curr. Protoc. Mol. Biol., 109: 21.29.1.

Capelle C.M., Zeng N., Danileviciute E., Rodrigues S.F., Ollert M., Balling R., He F.Q. (2021). Identification of VIMP as a gene inhibiting cytokine production in human $CD4^+$ effector T cells. iScience, 24: 102289.

Chhetri G., Liang Y., Shao J., Han D., Yang Y., Hou C., Wang P., Tao X., Shen Y., Jiang T., Feng L., Shen Y. (2020). Role of mesencephalic astrocyte-derived neurotrophic factor in alcohol-induced liver injury. Oxid. Med. Cell. Longev., 2020: 9034864.

Chrobociński K., Witarski W., Piórkowska K., (2022). A method of hepatocytes segmentation in microscopic images of trypan blue stained cellular suspension. Proc. Science and Information Conference, 2022, pp. 214–224.

Curran J.E., Jowett J.B.M., Elliott K.S., Gao Y., Gluschenko K., Wang J., Azim D.M.A., Cai G., Mahaney M.C., Comuzzie A.G., Dyer T.D., Walder K.R., Zimmet P., MacCluer J.W., Collier G.R., Kissebah A.H., Blangero J. (2005). Genetic variation in selenoprotein S influences inflammatory response. Nat. Genet., 37: 1234–1241.

Dudek J., Benedix J., Cappel S., Greiner M., Jalal C., Müller L., Zimmermann R. (2009). Functions and pathologies of BiP and its interaction partners. Cell. Mol. Life Sci., 66: 1556–1569.

Fernandes-da-Silva A., Miranda C.S., Santana-Oliveira D.A., Oliveira-Cordeiro B., Rangel-Azevedo C., Silva-Veiga F.M., Martins F.F., Souza-Mello V. (2021). Endoplasmic reticulum stress as the basis of obesity and metabolic diseases: focus on adipose tissue, liver, and pancreas. Europ. J. Nutr., 60: 2949–2960.

Fruman D.A., Mauvais-Jarvis F., Pollard D.A., Yballe C.M., Brazil D., Bronson R.T., Kahn C.R., Cantley L.C. (2000). Hypoglycaemia, liver necrosis and perinatal death in mice lacking all isoforms of phosphoinositide 3-kinase p85 alpha. Nat. Genet., 26: 379–382.

Gao Y., Feng H.C., Walder K., Bolton K., Sunderland T., Bishara N., Quick M., Kantham L., Collier G.R. (2004). Regulation of the selenoprotein SelS by glucose deprivation and endoplasmic reticulum stress – SelS is a novel glucose-regulated protein. FEBS Lett., 563: 185–190.

Iurlaro R., Muñoz-Pinedo C. (2016). Cell death induced by endoplasmic reticulum stress. FEBS J., 283: 2640–2652.

Jang S., Lee C.H. Choi K.M., Lee J., Choi J.W., Kim K.A., Park C.M. (2011). Correlation of fatty liver and abdominal fat distribution using a simple fat computed tomography protocol. World J. Gastroenterol., 17: 3335–3341.

Ji N., Xiang L., Zhou B., Lu Y., Zhang M. (2023). Hepatic gene expression profiles during fed–fasted–refed state in mice. Front. Genet., 14: 1145769.

Kampinga H.H., Craig E.A. (2010). The HSP70 chaperone machinery: J proteins as drivers of functional specificity. Nat. Rev. Mol. Cell Biol., 11: 579–592.

Kim Y.J., Kim H.J., Chung K.Y., Choi I., Kim S.H. (2014). Transcriptional activation of PIK3R1 by PPARγ in adipocytes. Mol. Biol. Rep., 41: 5267–5272.

Kuwabara K., Matsumoto M., Ikeda J., Hori O., Ogawa S., Maeda Y., Kitagawa K., Imuta N., Kinoshita T., Stern D.M., Yanagi H., Kamada T. (1996). Purification and characterization of a novel stress protein, the 150-kDa oxygen-regulated protein (ORP150), from cultured rat astrocytes and its expression in ischemic mouse brain. J. Biol. Chem., 271: 5025–5032.

Lee A.H., Scapa E.F., Cohen D.E., Glimcher L.H. (2008). Regulation of hepatic lipogenesis by the transcription factor XBP1. Science, 320: 1492–1496.

Lee J., Sun C., Zhou Y., Lee J., Gokalp D., Herrema H., Park S.W. Davis R.J., Ozcan U. (2011). p38 MAPK-mediated regulation of Xbp1s is crucial for glucose homeostasis. Nat. Med., 17: 1251–1260.

Lee J.H., Kwon J.H., Jeon Y.H., Ko K.Y., Lee S.R., Kim I.Y. (2014). Pro178 and Pro183 of selenoprotein S are essential residues for interaction with p97(VCP) during endoplasmic reticulum-associated degradation. J. Biol. Chem., 289: 13758–13768.

Lee J.H., Park K.J., Jang J.K., Jeon Y.H., Ko K.Y., Kwon J.H., Lee S.R., Kim I.Y. (2015). Selenoprotein S-dependent selenoprotein K binding to p97(VCP) protein is essential for endoplasmic reticulum-associated degradation. J. Biol. Chem., 290: 29941–29952.

Lin Y., Yang Z., Xu A., Dong P., Huang Y., Liu H., Li F., Wang H., Xu Q., Wang Y., Sun D., Zou Y., Zou X., Wang Yu, Zhang D., Liu H., Wu X., Zhang M., Fu Y., Cai Z., Liu C., Wu S. (2015). PIK3R1 negatively regulates the epithelial-mesenchymal transition and stem-like phenotype of renal cancer cells through the AKT/GSK3β/CTNNB1 signaling pathway. Sci. Rep., 5: 8997.

Lindholm P., Peränen J., Andressoo J.O., Kalkkinen N., Kokaia Z., Lindvall O., Timmusk T., Saarma M. (2008). MANF is widely expressed in mammalian tissues and differently regulated after ischemic and epileptic insults in rodent brain. Mol. Cell. Neurosci., 39: 356–371.

Liu X., Green R.M. (2019). Endoplasmic reticulum stress and liver diseases. Liver Res., 3: 55–64.

Liu J., Wu Z., Han D., Wei C., Liang Y., Jiang T., Chen L., Sha M., Cao Y., Huang F., Geng X., Yu J., Shen Yujun Wang H., Feng L., Wang D., Fang S., Wang S., Shen Y. (2020). Mesencephalic astrocyte-derived neurotrophic factor inhibits liver cancer through small ubiquitin-related modifier (SUMO)ylation-related suppression of NF-κB/Snail signaling pathway and epithelial-mesenchymal transition. Hepatology, 71: 1262–1278.

Liu X., Henkel A.S., LeCuyer B.E., Schipma M.J., Anderson K.A., Green R.M. (2015). Hepatocyte X-box binding protein 1 deficiency increases liver injury in mice fed a high-fat/sugar diet. Am. J. Physiol. Gastrointest. Liver Physiol., 309: G965–G974.

Love M.I., Huber W., Anders S. (2014). Moderated estimation of fold change and dispersion for RNA-seq data with DESeq2. Genome Biol., 15: 550.

Malhi H., Kaufman R.J. (2011). Endoplasmic reticulum stress in liver disease. J. Hepatol., 54: 795–809.

Milani P., Escalante-Chong R., Shelley B.C., Patel-Murray N.L., Xin X., Adam M., Mandefro B., Sareen D., Svendsen C.N., Fraenkel E. (2016). Cell freezing protocol suitable for ATAC-Seq on motor neurons derived from human induced pluripotent stem cells. Sci. Rep., 61: 1–10.

Mizobuchi N., Hoseki J., Kubota H., Toyokuni S., Nozaki J.I., Naitoh M., Koizumi A., Nagata K. (2007). ARMET is a soluble ER protein induced by the unfolded protein response via ERSE-II element. Cell Struct. Funct., 32: 41–50.

Park S.W., Zhou Y., Lee J., Lu A., Sun C., Chung J., Ueki K., Ozcan U. (2010). The regulatory subunits of PI3K, p85α and p85β, interact with XBP-1 and increase its nuclear translocation. Nat. Med., 16: 429–437.

Piórkowska K., Żukowski K., Ropka-Molik K., Tyra M. (2022). New long-non coding RNAs related to fat deposition based on pig model. Ann. Anim. Sci., 22: 1211–1224.

Pitts M.W., Hoffmann P.R. (2018). Endoplasmic reticulum-resident selenoproteins as regulators of calcium signaling and homeostasis. Cell Calcium, 70: 76–86.

Rao S., Oyang L., Liang J., Yi P., Han Y., Luo X., Xia L., Lin J., Tan S., Hu J., Wang H., Tang L., Pan Q., Tang Y., Zhou Y., Liao Q. (2021). Biological function of HYOU1 in tumors and other diseases. Onco. Targets. Ther., 14: 1727–1735.

Rehati A., Abuduaini B., Liang Z., Chen D., He F. (2023). Identification of heat shock protein family A member 5 (HSPA5) targets involved in nonalcoholic fatty liver disease. Genes Immun., 24: 124–129.

Ropka-Molik K., Pawlina-Tyszko K., Żukowski K., Tyra M., Derebecka N., Wesoły J., Szmatoła T., Piórkowska K. (2020). Identification of molecular mechanisms related to pig fatness at the transcriptome and miRNAome levels. Genes (Basel)., 11: 600.

Rueli R.H.L.H., Torres D.J., Dewing A.S.T., Kiyohara A.C., Barayuga S.M., Bellinger M.T., Uyehara-Lock J.H., White L.R., Moreira P.I., Berry M.J., Perry G., Bellinger F.P. (2017). Selenoprotein S reduces endoplasmic reticulum stress-induced phosphorylation of tau: potential role in selenate mitigation of tau pathology. J. Alzheimers. Dis., 55: 749–762.

Sanson M., Ingueneau C., Vindis C., Thiers J.C., Glock Y., Rousseau H., Sawa Y., Bando Y., Mallat Z., Salvayre R., Nègre-Salvayre A. (2008). Oxygen-regulated protein-150 prevents calcium homeostasis deregulation and apoptosis induced by oxidized LDL in vascular cells. Cell Death Differ., 15: 1255–1265.

Savell J.W., Cross H.R. (1988). The role of fat in the palatability of beef, pork, and lamb. Committee on Technological Options to Improve the Nutritional Attributes of Animal Products. National Academies Press (US).

Schulze A., Standera S., Buerger E., Kikkert M., Van Voorden S., Wiertz E., Koning F., Kloetzel P.M., Seeger M. (2005). The ubiquitin-domain protein HERP forms a complex with components of the endoplasmic reticulum associated degradation pathway. J. Mol. Biol., 354: 1021–1027.

Schweizer U., Fradejas-Villar N. (2016). Why 21? The significance of selenoproteins for human health revealed by inborn errors of metabolism. FASEB J., 30: 3669–3681.

Steensels S., Qiao J., Ersoy B.A. (2020). Transcriptional regulation in non-alcoholic fatty liver disease. Metabolites, 10: 1–34.

Sun Y., Cai R., Wang Y., Zhao R., Qin J., Pang W. (2020). A newly identified lncRNA LncIMF4 controls adipogenesis of porcine intramuscular preadipocyte through attenuating autophagy to inhibit lipolysis. Animals, 10: 926.

Tyra M., Zak G. (2013). Analysis of the possibility of improving the indicators of pork quality through selection with particular consideration of intramuscular fat (IMF) content. Ann. Anim. Sci., 13: 33–44.

Ueki K., Algenstaedt P., Mauvais-Jarvis F., Kahn C.R. (2000). Positive and negative regulation of phosphoinositide 3-kinase-dependent signaling pathways by three different gene products of the p85alpha regulatory subunit. Mol. Cell. Biol., 20: 8035–8046.

Vickers A.E.M., Ulyanov A.V., Fisher R.L. (2018). Progression of repair and injury in human liver slices. Int. J. Mol. Sci., 19: 4130.

Wang D.Q., Miao X., Gao J., Zhou Y., Ji F., Cheng X. (2019). The 150-kDa oxygen-regulated protein (ORP150) regulates proteinuria in diabetic nephropathy via mediating VEGF. Exp. Mol. Pathol., 110: 104255.

Wang J., Lee J., Liem D., Ping P. (2017). HSPA5 Gene encoding Hsp70 chaperone BiP in the endoplasmic reticulum. Gene, 618: 14–23.

Wang M., Wey S., Zhang Y., Ye R., Lee A.S. (2009). Role of the unfolded protein response regulator GRP78/BiP in development, cancer, and neurological disorders. Antioxid. Redox Signal., 11: 2307–2316.

Wang M., Zhang J., Gong N. (2022). Role of the PI3K/Akt signaling pathway in liver ischemia reperfusion injury: a narrative review. Ann. Palliat. Med., 11: 806–817.

Xiao G., Zhang T., Yu S., Lee S., Calabuig-Navarro V., Yamauchi J., Ringquist S., Dong H.H. (2013). ATF4 protein deficiency protects against high fructose-induced hypertriglyceridemia in mice. J. Biol. Chem., 288: 25350–25361.

Xing K., Wang K., Ao H., Chen S., Tan Z., Wang Y., Xitong Z., Yang T., Zhang F., Liu Y., Ni H., Sheng X., Qi X., Wang X., Guo Y., Wang C. (2019). Comparative adipose transcriptome analysis digs out genes related to fat deposition in two pig breeds. Sci. Rep., 9: 1–11.

Yan F., Powell D.R., Curtis D.J., Wong N.C. (2020). From reads to insight: a hitchhiker's guide to ATAC-seq data analysis. Genome Biol., 21: 1–16.

Yang C., Gao Y. (2020). Mesencephalic astrocyte-derived neurotrophic factor: A treatment option for Parkinson's disease. Front. Biosci., 25: 1718–1731.

Yang W., Shen Y., Chen Y., Chen L., Wang L., Wang H., Xu S., Fang S., Fu Y., Yu Y., Shen Yuxian (2014). Mesencephalic astrocyte-derived neurotrophic factor prevents neuron loss via inhibiting ischemia-induced apoptosis. J. Neurol. Sci., 344: 129–138.

Ye Y., Shibata Y., Yun C., Ron D., Rapoport T.A., Ye Y., Shibata Y., Yun C., Ron D., Rapoport T.A. (2004). A membrane protein complex mediates retro-translocation from the ER lumen into the cytosol. Nature, 429: 841–847.

Yoshiuchi K., Kaneto H., Matsuoka T., Kohno K., Iwawaki T., Nakatani Y., Yamasaki Y., Hori M., Matsuhisa M. (2008). Direct monitoring of in vivo ER stress during the development of insulin resistance with ER stress-activated indicator transgenic mice. Biochem. Biophys. Res. Commun., 366: 545–550.

Zong Z.H., Du Z.X., Zhang H.Y., Li C., An M.X., Li S., Yao H.B., Wang H.Q. (2016). Involvement of Nrf2 in proteasome inhibition-mediated induction of ORP150 in thyroid cancer cells. Oncotarget, 7: 3416–3426.

Received: 17 VI 2024
Accepted: 2 XII 2024